



## Molecular Crystals and Liquid Crystals

Publication details, including instructions for authors and subscription information:

<http://www.tandfonline.com/loi/gmcl20>

## Photoinduced Spatial Orientational Order in Methacrylic Azopolymers

Oksana Nadtoka<sup>a</sup>, Vladimir Syromyatnikov<sup>a</sup>, Lidiya Olkhovik<sup>a</sup>, Oleg Yaroshchuk<sup>b</sup> & Tetyana Bidna<sup>b</sup>

<sup>a</sup> Taras Shevchenko Kyiv National University, Kyiv, Ukraine

<sup>b</sup> Institute of Physics, NASU, Kyiv, Ukraine

Version of record first published: 22 Sep 2010

To cite this article: Oksana Nadtoka, Vladimir Syromyatnikov, Lidiya Olkhovik, Oleg Yaroshchuk & Tetyana Bidna (2007): Photoinduced Spatial Orientational Order in Methacrylic Azopolymers, *Molecular Crystals and Liquid Crystals*, 468:1, 63/[415]-76/[428]

To link to this article: <http://dx.doi.org/10.1080/15421400701229487>

PLEASE SCROLL DOWN FOR ARTICLE

Full terms and conditions of use: <http://www.tandfonline.com/page/terms-and-conditions>

This article may be used for research, teaching, and private study purposes. Any substantial or systematic reproduction, redistribution, reselling, loan, sub-licensing, systematic supply, or distribution in any form to anyone is expressly forbidden.

The publisher does not give any warranty express or implied or make any representation that the contents will be complete or accurate or up to

date. The accuracy of any instructions, formulae, and drug doses should be independently verified with primary sources. The publisher shall not be liable for any loss, actions, claims, proceedings, demand, or costs or damages whatsoever or howsoever caused arising directly or indirectly in connection with or arising out of the use of this material.



## Photoinduced Spatial Orientational Order in Methacrylic Azopolymers

**Oksana Nadтока**

**Vladimir Syromyatnikov**

**Lidiya Olkhovik**

Taras Shevchenko Kyiv National University, Kyiv, Ukraine

**Oleg Yaroshchuk**

**Tetyana Bidna**

Institute of Physics, NASU, Kyiv, Ukraine

*The combination of the transmission null ellipsometry and the total absorption method is applied to study the 3D orientational configurations of azochromophores in polymethacrylates with azobenzene side groups. The transformation of the initial orientation due to the photoexcitation of azochromophores is investigated. Under irradiation, if the reorientation mechanism of the photoinduced ordering prevails, the azochromophores are reoriented perpendicularly to the polarization direction of the exciting light,  $E_{ex}$ . In the case where the photoselection ordering mechanism dominates, the 3D distribution of azochromophores in the saturation state of irradiation is isotropic due to a strong exhaustion of the number of anisotropic trans isomers. The observed regularities were earlier described for several other classes of photosensitive polymers, and so they may be common rules for the photoordering in photochromic media.*

**Keywords:** azopolymer; photoinduced anisotropy; polymethacrylate; 3D orientational order

### 1. INTRODUCTION

Azobenzene and its derivatives have attracted a much attention over the past few decades because of a number of fascinating features of

These studies were carried out within the framework of the project “Ordering regularities and properties of nano-composite systems” of the NAS of Ukraine. Partially, they were also supported by INTAS (project No 03-51-5448).

Address correspondence to Oksana Nadтока, Kyiv National Taras Shevchenko University, Volodymyrs'ka St., 64, Kyiv 01033, Ukraine. E-mail: oksananadtoka@ukr.net

these compounds. They were initially used for the preparation of paints, because of a rich spectrum of colors that can be obtained depending on the chemical structure of azochromophores. Further investigations revealed the strong photochromism of azobenzene derivatives. It was found that this effect in azobenzene derivatives can be accompanied by the novel phenomenon that is known as photoinduced optical anisotropy (POA) and can be detected in dichroism and birefringence measurements [1]. This feature makes azopolymers rather attractive for a number of photonic applications such as polarization holography, optical memory, integrated optical circuits, and liquid crystal (LC) aligning substrates, etc. [2,3].

On the microscopic level, POA in azopolymers is explained by the orientational ordering of azochromophores. The widely accepted model of this photoorientation is based on the specific photochemistry (*trans-cis* isomerization) and the strong absorption dichroism of azochromophores in the *trans* configuration. According to theory of Dumont [4,5], the mechanism of POA is determined by the molecular extinctions (along the long and short molecular axes) of *trans* and *cis* azochromophores depending on the wavelength of excitation, lifetime of *cis* isomers, and the coefficient of rotational diffusion. M. Dumont selected two elementary mechanisms. The first mechanism, *photoselection or angular hole burning*, is realized if the lifetime of *cis* isomers is long, while their molecular extinction is low, so that azochromophores undergo only one or few cycles of isomerization over the irradiation period. Under these conditions, if the rotational diffusion rate is not very high, the anisotropic distribution of azochromophores appears due to the angularly selective conversion of *trans* chromophores into the less anisotropic (isotropic in the first approximation) *cis* form. The strongest conversion is observed for the fragments oriented along the polarization direction of the exciting light,  $\mathbf{E}_{\text{ex}}$ . So, due to the photoselection, azochromophores will be mainly aligned perpendicularly to  $\mathbf{E}_{\text{ex}}$ . If photoproducts are thermally and photochemically stable, the hole burning saturation leads to a total depletion of the *trans* form and so to the isotropy of an azopolymer film. In the opposite case, if the lifetime of *cis* isomers is short and/or their molecular extinction is high, azochromophores undergo many isomerization cycles over the excitation period. The change of the molecular shape leads to a change of the molecular orientation. Due to the many cycles of isomerization, a random-walk rotation of an azochromophore appears. The chromophores accidentally aligned perpendicularly to  $\mathbf{E}_{\text{ex}}$  will be excluded from the further rotation, because their absorption is minimized. Thus, the photoinitiated random-walk rotation leads to the accumulation of azochromophores in the direction perpendicular to the

polarization of the exciting light. This mechanism is known as *photo-reorientation* or *angular redistribution*. More generally, through both the photoselection and photoreorientation, the system tends to minimize the probability of the optical excitation. The final distribution of azochromophores is a result of the competition between the above ordering process and the thermal diffusion in the ground state, which tends to establish the isotropy.

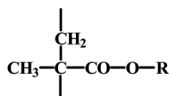
In the present research, we elucidate the ordering regularities in azogroups contained in polymethacrylates (poly-AzoMA). This is the most popular class of azopolymers quite attractive for practical uses because of the enhanced thermal stability, excellent film-forming properties, relatively simple synthesis, *etc.* In spite of this popularity, the studies of the photoinduced anisotropy in these polymers were mainly restricted to the 2D case, which cannot give a complete idea of the ordering peculiarities. Regarding the 3D consideration, we note only a few studies based on different variations of the prism coupling method [4,6,7] and works of Spiess with coworkers [8] used the total absorption method briefly described in the following section. In addition, the 3D order in a polymer of this class has been studied in our previous works [9–11]. In the present paper, we apply the transmission null ellipsometry supported by the modified total absorption method to investigate the 3D order in a big series of azopolymers based on polymethacrylate. As we earlier proved, this combination is effective practical tool for the study of orientational molecular distributions. We consider the induced orientational order as a function of the molecular structure, supramolecular organization, and irradiation conditions. The regularities obtained are compared with those earlier established for other kinds of azopolymers.

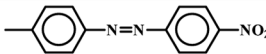
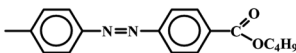
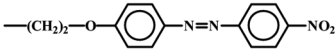
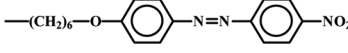
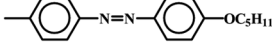
## 2. EXPERIMENTAL

### 2.1. Materials

The general structure of poly-AzoMA is shown in Chart 1. All the chemicals were purchased from commercial suppliers and used without further purification unless otherwise noted. Standard distillation procedures were applied. The structures of all the precursors and final products were confirmed by  $^1\text{H}$  NMR spectroscopy of solutions. All  $^1\text{H}$  NMR spectra were taken in  $\text{CDCl}_3$ . The synthesis of all polymers was similar, and only the steps toward making poly-AzoMA are detailed.

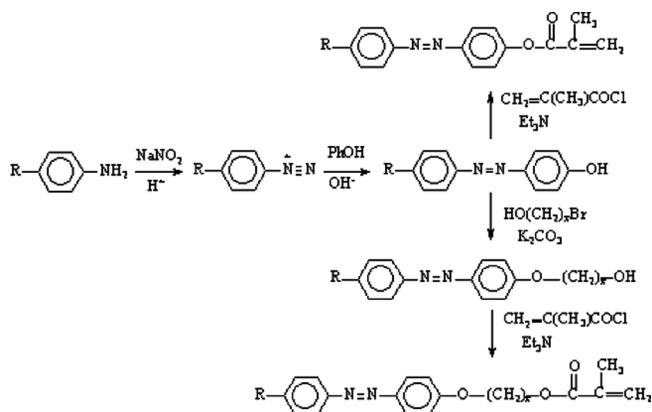
**Monomer synthesis.** The synthesis route for the target azomonomers (M) is shown in Scheme 1. The corresponding monomers were synthesized by general methods. The azocompound (0.06 mol) and



Code	R	T <sub>g</sub> , °C	λ <sub>max</sub> , nm	M <sub>n</sub>	M <sub>w</sub>	M <sub>w</sub> /M <sub>n</sub>
P1		160	350	5600	7780	1,39
P2		123	350	1500	1900	1,26
P3		113	355	4020	5580	1,39
P4		112	362	3000	4140	1,39
P5		123	348	2000	2450	1,24

**CHART 1** Objects of Investigation (p-AzoMA).

triethylamine (9.0 mL) were dissolved in THF (200 mL). The solution was kept in an ice bath for 10 min. A solution of distilled methacryloyl chloride (6.0 mL, 0.06 mol) was added slowly to the above mixture. After the addition of methacryloyl chloride, the resulting mixture

**SCHEME 1** Synthesis of methacrylic azomonomers.

was stirred at room temperature overnight. Then the solution was poured into distilled water (1 L), and the obtained residue was filtered and air-dried. Recrystallization of monomers was carried out in ethanol.

**4'-methacryloxy-4-nitroazobenzene (M1).** Orange crystals; yield 69%; mp 145°C (by DSC).  $^1\text{H}$  NMR ( $\text{CDCl}_3$ ),  $\delta$  (ppm): 8.43 (d, 2H, Ph-H *ortho* to  $\text{NO}_2$ ), 8.07 (d, 2H, Ar), 8.03 (d, 2H, Ar), 7.40 (d, 2H, Ar), 6.34 (s, 1H,  $=\text{CH}_2$ ), 5.91 (s, 1H,  $=\text{CH}_2$ ), 2.05 (s, 3H,  $-\text{CH}_3$ ). UV-vis (Ethanol)  $\lambda_{\text{max}}$ : 360, 485 nm. Elem. Anal. Calcd for  $\text{C}_{16}\text{H}_{13}\text{O}_4\text{N}_3$ : C, 61.74%, H, 4.18%; N, 13.50%. Found: C, 61.70%, H, 4.16%; N, 13.52%.

**4'-methacryloxyethyloxy-4-nitroazobenzene (M2).** Orange crystals; yield 56%; mp 130°C (by DSC).  $^1\text{H}$  NMR ( $\text{CDCl}_3$ ),  $\delta$  (ppm): 8.00 (d, 2H, Ar), 8.37 (d, 2H, Ar), 7.62 (d, 2H, Ar), 7.13 (d, 2H, Ar), 6.4 (s, 1H,  $=\text{CH}_2$ ), 5.8 (s, 1H,  $=\text{CH}_2$ ), 2.15 (s, 3H,  $-\text{CH}_3$ ), 4.10 (m, 2H,  $\text{ArOCH}_2$ ), 1.72 (m, 2H,  $\text{OCH}_2$ ). UV-vis (ethanol)  $\lambda_{\text{max}}$ : 360, 490 nm. Elem. Anal. Calcd for  $\text{C}_{18}\text{H}_{17}\text{O}_5\text{N}_3$ : C, 60.85%, H, 4.79%; N, 11.83%. Found: C, 60.88%, H, 4.81%; N, 11.85%.

**4'-methacryloxyhexyloxy-4-nitroazobenzene (M3).** Orange crystals; yield 50%; mp 72°C (by DSC).  $^1\text{H}$  NMR ( $\text{CDCl}_3$ ),  $\delta$  (ppm): 8.02 (d, 2H, Ar), 8.34 (d, 2H, Ar), 7.68 (d, 2H, Ar), 7.10 (d, 2H, Ar), 6.30 (s, 1H,  $=\text{CH}_2$ ), 5.95 (s, 1H,  $=\text{CH}_2$ ), 2.20 (s, 3H,  $-\text{CH}_3$ ), 4.10 (m, 2H,  $\text{ArOCH}_2$ ), 3.9 (m, 2H,  $\text{HOCH}_2$ ), 1.72 (m, 4H,  $\text{H}_2$ ). UV-vis (ethanol)  $\lambda_{\text{max}}$ : 365, 490 nm. Elem. Anal. Calcd for  $\text{C}_{22}\text{H}_{25}\text{O}_5\text{N}_3$ : C, 61.74%, H, 4.18%; N, 13.50%. Found: C, 61.70%, H, 4.16%; N, 13.52%.

**4'-methacryloxy-4-butoxycarbonylazobenzene (M4).** Yellow crystals; yield 60%; mp 63°C (by DSC).  $^1\text{H}$  NMR ( $\text{CDCl}_3$ ),  $\delta$  (ppm): 7.89 (d, 2H, Ar), 7.73 (d, 2H, Ar), 7.93 (d, 2H, Ar), 6.94 (d, 2H, Ar), 6.34 (s, 1H,  $=\text{CH}_2$ ), 5.90 (s, 1H,  $=\text{CH}_2$ ), 2.10 (s, 3H,  $-\text{CH}_3$ ), 4.17 (m, 2H,  $\text{CH}_2$ ), 1.72 (m, 9H,  $\text{C}_4\text{H}_9$ ). UV-vis (ethanol)  $\lambda_{\text{max}}$ : 363, 495 nm. Elem. Anal. Calcd for  $\text{C}_{21}\text{H}_{22}\text{O}_4\text{N}_2$ : C, 67.38%, H, 5.88%; N, 7.65%. Found: C, 67.40%, H, 5.90%; N, 7.61%.

**4'-methacryloxy-4-pentoxiazobenzene (M5).** Yellow crystals; yield 65%; mp 72°C (by DSC).  $^1\text{H}$  NMR ( $\text{CDCl}_3$ ),  $\delta$  (ppm): 7.85 (d, 2H, Ar), 7.65 (d, 2H, Ar), 7.74 (d, 2H, Ar), 6.91 (d, 2H, Ar), 6.30 (s, 1H,  $=\text{CH}_2$ ), 5.84 (s, 1H,  $=\text{CH}_2$ ), 2.08 (s, 3H,  $-\text{CH}_3$ ), 4.2 (m, 2H,  $\text{CH}_2$ ), 1.72 (m, 9H,  $\text{C}_4\text{H}_9$ ). UV-vis (ethanol)  $\lambda_{\text{max}}$ : 378, 500 nm. Elem. Anal. Calcd for  $\text{C}_{21}\text{H}_{24}\text{O}_3\text{N}_2$ : C, 71.59%, H, 6.82%; N, 7.95%. Found: C, 71.62%, H, 6.80%; N, 7.93%.

**Polymerization.** Homopolymers were synthesized by free-radical polymerization in toluene. The polymerization was carried out in a 10-wt.% toluene solution of the monomer with AIBN as a free radical initiator (10 wt.% of the monomer) at 80°C over more than 30 h. Polymers were isolated from the reaction solution by precipitation into the

excess of methanol followed by reprecipitation from toluene into methanol and then dried at 20°C overnight. The synthesis is described in more details in a separate paper [12].

The synthesized azopolymers were characterized by  $^1\text{H}$  NMR spectroscopy. The obtained results were in agreement with the proposed structures.

The phase transitions were studied by differential scanning calorimetry (DSC) using a Perkin Elmer DSC-2 instrument equipped with an IFA GmbH processor at a scan rate of 20° K/min. The calorimetry calibration was carried out according to the well-known recent recommendation [13–15] using sapphire and quartz as the standard.

## 2.2. Films

The polymers were dissolved in DMF (2 wt%) and filtered by using a 0.2  $\mu\text{m}$  Teflon filters. The prepared solution was spin coated on the plates of fused quartz allowing us to measure the polymer absorption in a UV range. The films were dried at 90°C for 1 h. The thickness of the films was measured by a profilometer. It was varied within 300–1000 nm.

The photo-ordering processes were initiated with the polarized UV light from a high-pressure mercury lamp. The light propagation direction corresponded to the  $z$ -axis, while the light polarization was always chosen along the  $x$ -axis of the Cartesian coordinate system with the  $x$ - and  $y$ -axes parallel to the verges of a rectangular polymer film, the  $z$ -axis being normal to this film (Fig. 1). The line at 365 nm was selected with an interference filter. The light was directed normally to the films. The irradiation was carried out stepwise. After each irradiation step, the photoinduced order was evaluated. The time period between the irradiation and measurements was about 10 min to ensure the relaxation of *cis* isomers (at least their short living fraction).

## 2.3. Methods

The key method of our studies was the *transmission null ellipsometry (TNE)*. This is a modified version of the Senarmon method extended for measurements of the out-of-plane retardation. The obtained in-plane and out-of-plane retardation values ( $(n_y - n_x)d$  and  $(n_z - n_x)d$ , Fig. 1) allowed us to judge about the ellipsoid of the refractive index  $n_{ij}$  and, finally, about the orientational configuration of azochromophores assuming that the directions of maximal values of  $n_{ij}$  correspond to the maximally populated directions of azochromophores. The details of this method can be found in our previous works [9,10].



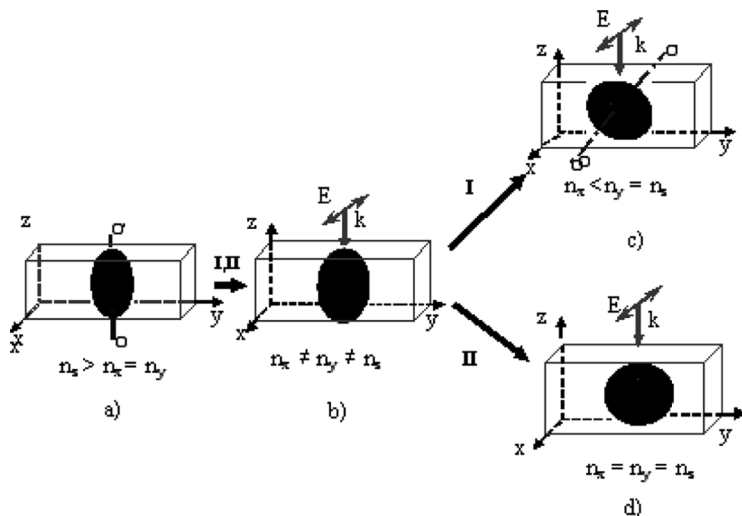


**FIGURE 1** The transformations of the 3D orientational distributions of *trans*-azochromophores in the poly-AzoMA films due to  $\lambda = 365$  nm irradiation. (a) before irradiation; (b) biaxial transient distribution; (c) oblate distribution with the symmetry axis parallel to  $\mathbf{E}_{\text{ex}}$  (P1, P2, P3, P4, photosaturation state); (d) isotropic distribution (P5, photosaturation state).

As a complementary characterization method, we also perform 2D dichroism measurements in the UV/Visible spectral range. The optical densities,  $D_x$  and  $D_y$ , corresponding to the  $x$  and  $y$  in-plane polarizations, are measured with a probe beam propagating perpendicularly to the sample. The third out-of-plane component  $D_z$ , can be estimated by the *total absorption (TA) method*, if the total absorption,  $D_{\text{total}} = D_x + D_y + D_z$ , is the same for all measuring steps. This is true, for instance, if the photoinduced *cis* isomers quickly relax back to the *trans* form and the loss of azochromophores due to a photodegradation is negligible. The  $D_{\text{total}}$  can be easily obtained, if the sample is uniaxial at some instant of time  $t_0$  with an in-plane orientation of the anisotropy axis, say  $y$ . Then

$$D_{\text{total}} \equiv D_x(t_0) + D_y(t_0) + D_z(t_0) = 2D_x(t_0) + D_y(t_0) \quad (1)$$

Since we assumed that the number of azobenzene units in the *trans* configuration remains constant at each instant of time  $t$ ,  $D_z(t)$  can be estimated as

$$D_z(t) = D_{\text{total}} - D_x(t) - D_y(t), \quad (2)$$

where  $D_x(t)$  and  $D_y(t)$  are the experimentally measured in-plane components.

Then, the diagonal terms of the tensor of orientational order  $S_{ij}$  can be estimated. For example:

$$S_{xx} = \frac{D_x - \frac{1}{2}(D_y + D_z)}{D_x + D_y + D_z}. \quad (3)$$

The components  $S_{yy}$  and  $S_{zz}$  can be obtained by cyclic permutation in expression (3).

In the original version of TAM,  $D_i (i = x, y, z)$  corresponded to the maximum of the vibration bands (IR spectral range) characteristic of azochromophore. In our version, the absorption in the UV/Vis range is measured. We operated with the  $D_i (i = x, y, z)$  values corresponding to the  $\pi\pi^*$  absorption maximum of *trans* chromophores.

The UV/Vis absorption measurements were carried out by using a diode array spectrometer S2000 from Ocean Optics Co. The samples were set normally to the testing light from a low-intensity deuterium lamp. A Glan-Thompson prism was used to polarize the probe beam.

## RESULTS AND DISCUSSION

First of all, we measured the UV/Vis absorption spectra of azopolymers before and after the irradiation with the unpolarized UV light (365 nm, normal incidence). These measurements confirmed that the major photoreaction is the *trans-cis* isomerization revealed itself in a strong depletion of the  $\pi\pi^*$  band and an increase of the  $n\pi^*$  band which is much more intense for *cis* isomers. The  $\lambda_{\pi\pi^*}$  values corresponding to a maximum of the  $\pi\pi^*$  absorption band are shown in Chart 1. As usually, a bathochromic shift of the  $\pi\pi^*$  band is observed by substituting the alkoxy chain by a polar  $\text{NO}_2$  group in the chromophore's tail (push-pull chromophores). In spite of this shift, the 365-nm excitation wavelength corresponds in all polymers to the effective adsorption within the  $\pi\pi^*$  absorption band.

With regard for the results on the 3D ordering, two types of the ordering behavior can be selected. We describe them by an example of P1 and P5, representatives of these two types. The values of the in-plane,  $(n_y - n_x)d$ , and the out-of-plane  $(n_z - n_x)d$  retardation for the films of P1 and P5 are presented, respectively, in Figure 2a and Fig. 3a. The data correspond to successive exposure doses (the  $x$  polarization of the UV irradiation). Several conclusions from these curves can be drawn. First of all, before the irradiation,

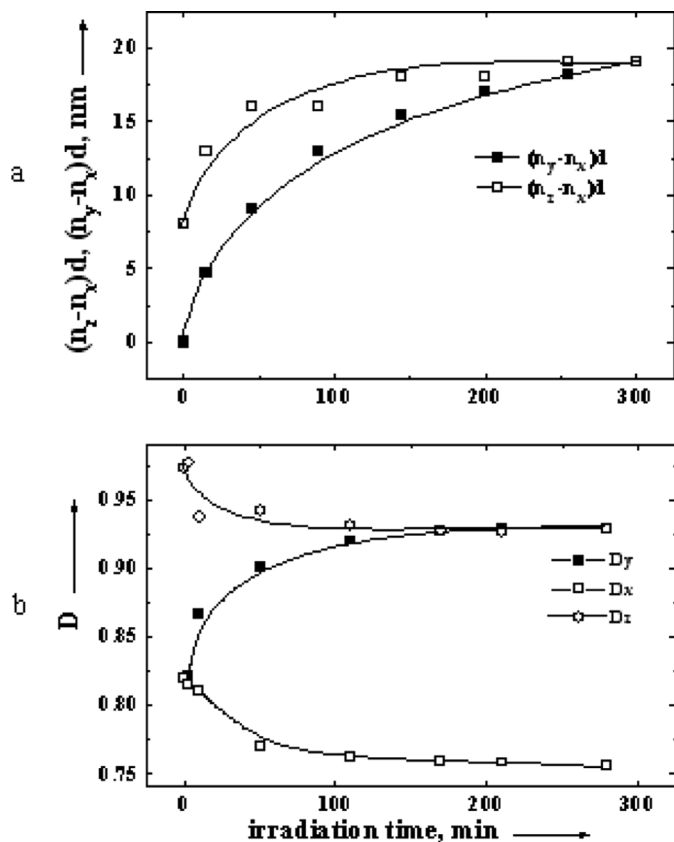


**FIGURE 2** Dependence of the absorption components (a) and phase retardation components (b) of polymer P1 on irradiation time under conditions: the wavelength was 365 nm, the intensity was 5 mW/cm<sup>2</sup>, x polarization).

azochromophores demonstrate a slight preference to the out-of-plane alignment ( $n_z > n_x = n_y$ , Fig. 1a). This rule was true for all homologues studied. The irradiation, however, induces different kinds of a transformation of this initial order in two different polymer classes we selected. This difference is especially clear for the structures realized in the saturated states of the irradiation reached for all polymers. In the P1 film, the irradiation results in an oblate order with the  $x$  ordering axis ( $n_x < n_y = n_z$ , Fig. 1c). In contrast, in the P5 film, the isotropic order is formed ( $n_x = n_y = n_z$ , Fig. 1d). In the general case, the transient orientational structures are biaxial ( $n_x \neq n_y \neq n_z$ , Fig. 1b). In P5 films, between the biaxial and isotropic orientations, the uniaxial out-of-plane alignment ( $n_z > n_x = n_y$ , Fig. 1a) can be observed as a

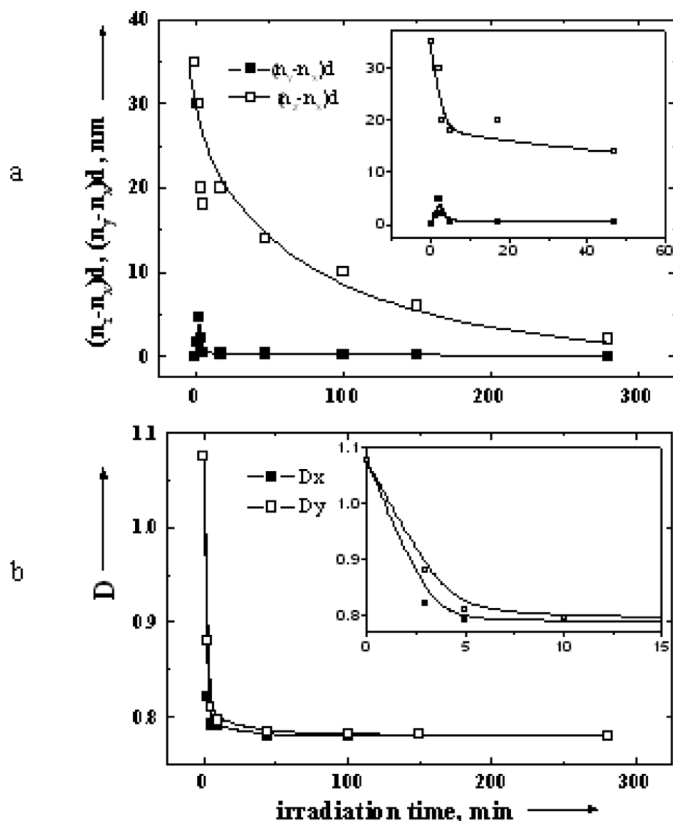


**FIGURE 3** The kinetics of the absorption components  $D_x, D_y$  (a) and phase retardation components  $(n_y - n_x)d$  and  $(n_z - n_x)d$  (b) for successive exposure doses for polymer P5. Irradiation is with  $\lambda_{\text{ex}} = 365$  nm ( $I = 5$  mW/cm<sup>2</sup>, x polarization).

result of the faster degradation of the in-plane anisotropy  $(n_y - n_x)d$  compared with the out-of-plane anisotropy  $(n_z - n_x)d$ . The  $D_x$  and  $D_y$  absorption components as functions of the exposure time measured for P1 and P5 are presented in Figure 2b and Figure 3b. The behavior of the  $D_x(t)$  and  $D_y(t)$  curves in Figure 2b is typical of the reorientation mechanism: an increase of  $D_y(t)$  and a simultaneous decrease of  $D_x(t)$  ( $x \parallel \mathbf{E}_{\text{ex}}$ ) is an evidence for the redistribution of azochromophores with increase of their concentration in the  $y$  direction perpendicular to the light polarization  $\mathbf{E}_{\text{ex}}$  [4,5]. In turn, the simultaneous decrease of  $D_x(t)$  and  $D_y(t)$  curves is typical of the angular photoselection [4,5]. The conversion of *trans* isomers in the long living *cis* form firstly in

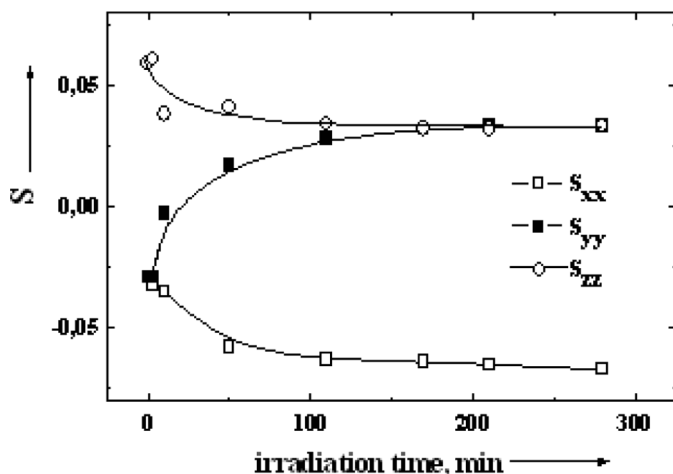


**FIGURE 4** Kinetics of  $S_{xx}$ ,  $S_{yy}$ ,  $S_{zz}$  for successive exposure doses (polymer P1) calculated from the data of Fig. 2 b according to formula (3).

the light polarization direction  $\mathbf{E}_{ex}$  and then in all other spatial directions may explain the isotropic order realized in the P5 film at high irradiation doses.

As we discussed in Introduction, the reorientation mechanism may be an evidence for the short lifetime of *cis* isomers. If it is really so, the total absorption of azochromophores  $D_{total}$  can be practically kept constant after successive irradiation steps. In conjunction with a fact of the uniaxial ordering in a stationary state ( $n_y = n_z$ ), this allows us to apply the TA method to calculate the  $D_z$  component. The calculated  $D_z(t)$  curve is shown in Figure 2b.

The  $D_i(i = x, y, z)$  values were used to calculate the diagonal components  $S_{xx}$ ,  $S_{yy}$ , and  $S_{zz}$  of the order parameter tensor  $\hat{S}$  according to (3). The  $S_{xx}(t)$ ,  $S_{yy}(t)$ , and  $S_{zz}(t)$  curves are shown in Figure 4. The uniaxial oblate distribution of azochromophores with the  $x$  ordering axis, realized in the stationary state of irradiation, is characterized by the scalar  $S \equiv S_{xx} = -0.07$ . The initial order of azochromophores (uniaxial ordering along the film normal) is also characterized by a scalar:  $S \equiv S_{zz} = 0.06$ . The latter value indicates that the initial out-of-plane ordering is rather weak. The transient structures between the uniaxial structures in the initial state and in the stationary state of the excitation are biaxial and so can be described at least with three (diagonal) elements of  $\hat{S}$ .

Note again, that the TA method cannot be applied for P5 because of the strong exhaustion of *trans* chromophores possible for rather stable

*cis* isomers. This automatically excludes the conditions needed for the TA method.

Qualitatively, the ordering peculiarities of P1 inhere in the series P2, P3, P4, i.e., in all homologues containing an acceptor group (push-pull azochromophore). The transformation of the 3D order under irradiation for these polymers is schematically presented in Fig. 1 as transformation way I. This general tendency does not depend on the length of the side-chain spacer as well as on the concentration of azochromophores in co-polymers. At the same time, the mentioned molecular variations influence the induced birefringence and dichroism which determine the ordering rate of azochromophores. These quantitative regularities will be considered in the forthcoming publications.

The ordering features of P5 are presented as transformation way II in Fig. 1: on the initial stage of irradiation, the biaxial alignment is observed, which transforms, with increase in the irradiation dose, into a spatially isotropic distribution.

The general tendencies of the photoinduced ordering allows us to conclude that the photoinduced order in poly-AzoMA is mainly influenced by the molecular photoordering through the photoselection and reorientation mechanisms described above. The clear evidence for it is the fact that the realized orientational configurations of azochromophores reflect the photoexcitation geometry. Energetically, these configurations can be not profitable (as in our experimental case), counter to a self-organization of anisotropic molecules aimed at the achievement of a uniaxial prolate order to minimize the free energy of a polymer. So, in strong contrast to azobenzene polyesters earlier studied [16], the self-ordering under photoirradiation in poly-AzoMA at the ambient temperatures is rather weak. This can be caused by rather high temperatures of the glass transition ( $T_g > 100^\circ\text{C}$ ), which testifies to a deep “freezing” of p-AzoMA chains, so that they cannot be involved in the processes of self-organization stimulated by UV light. Contrary to this, the glass transition temperatures in azopolyesters are low ( $T_g < 20^\circ\text{C}$ ). So both azochromophores and polyester chains participate in the collective processes of self-organization. The “freezing” of polymer chains in poly-AzoMA polymers can also explain why the liquid crystallinity, as a particular feature of the self-organization, does not influence substantially the order in these polymers. According to [17], the contribution of the intrinsic self-organization to the orientational order in poly-AzoMA can be strongly increased if the film is irradiated at a temperature a little lower than  $T_g$ . Thus, the competition of the molecular photoorientation and the self-organization in the 3D ordering can be achieved for

elevated temperatures close to 100°C. This can be a rather interesting subject for the future studies.

Since a light ordering factor at ambient temperatures strongly prevails, the induced orientation depends rather on the molecular photochemistry than on the self-ordering processes. If the photoreorientation mechanism dominates, the oblate order with the symmetry axis parallel to  $\mathbf{E}_{\text{ex}}$  is formed. In the opposite case, if the photoselection mainly influences the order, a spatially isotropic alignment is realized.

## CONCLUSIONS

Thus, studying the 3D orientational ordering in the azogroups containing polymethacrylates, we revealed the regularities earlier established for other kinds of azopolymers [16], as well as the polymers containing a cinnamoyl photosensitive group [18]. The main rule says that, under photoexcitation, the initial orientational distribution (frequently, it is uniaxially ordered due to the self-ordering of photosensitive groups) is transformed into some other uniaxially ordered distribution (in the case of the photoreorientation mechanism) or the isotropic distribution (in the case of photoselection). The transient structures from the initial to the final uniaxial (isotropic) distributions are biaxial. In the case of photoselection, the transient uniaxial homeotropic alignment can be observed if the in-plane depletion rate of *trans* chromophores is substantially higher than the out-of-plane one. Before the irradiation, the azochromophores in the studied poly-AzoMA demonstrate the preference to the out-of-plane alignment that can be caused by the self-ordering in the diluted polymers under the film formation. The final photoinduced alignment is a result of the concurring photoorientation and the self-organization. The latter factor in poly-AzoMA at ambient temperatures is weak, presumably, because of high  $T_g$ . This does not allow the collective self-organization processes under photoexcitation to play an important role, for example, in azopolyesters [19]. The regularities observed may predict the alignment tendencies in other kinds of photopolymers showing POA.

## REFERENCES

- [1] Weigert, F. (1919). *Verh. Dtsch. Phys. Ges.*, 21, 479.
- [2] Xie, S., Natansohn, A., & Rochon, P. (1993). *Chem.Mater.*, 5, 403.
- [3] Shibaev, V. P. *et al.* (1996). *Polymers as Electrooptical and Photooptical Active Media*, Springer: New York.
- [4] Dumont, M. & Sekkat, Z. (1992). *Proc SPIE.*, 188, 1774.
- [5] Dumont, M. (1996). *Mol. Cryst. Liq. Cryst.*, 282, 437.

- [6] Cimrova, V., Neher, D., Kostromine, S., & Bieringer, Th. (1999). *Macromolecules*, 32, 8496.
- [7] Jung, C., Rutloh, M., & Stumpe, J. (2002). *Mol. Cryst. Liq. Cryst.*, 375, 713.
- [8] Wiesner, U., Reynolds, N., Boeffel, Ch., & Spiess, H. W. (1992). *Liq. Crystals*, 11, 251.
- [9] Yaroshchuk, O., Sergan, T., Lindau, J., Lee, S. N., Kelly, J., & Chien, L.-C. (2001). *J. Chem. Phys.*, 114, 5330.
- [10] Yaroshchuk, O., Kiselev, A., Zakrevskyy, Yu., Stumpe, J., & Lindau, J. (2001). *Eur. Phys. J. E*, 6, 57.
- [11] Yaroshchuk, O. V., Kiselev, A. D., Zakrevskyy, Yu. A., Bidna, T. V., Kelly, J., Chien, L.-C., & Lindau, J. (2003). *Phys. Rev. E*, 68(1), 011803.
- [12] Nadtoka, O., Syromyatnikov, V., & Olkhovykh, L. (2005). *Mol. Cryst. Liq. Cryst.*, 427, 259.
- [13] Wunderlich, B., Boller, A., Okazaki, I., & Ishikiriya, K. (1997). *Thermochim. Acta*, 304–305, 125.
- [14] Ribeiro, M., Grolier, J. -P. E. (1999). *J. Thermal Anal. & Calorimetry*, 57, 253.
- [15] Wunderlich, B. (2003). *Prog. Polymer Sci.*, 28, 383.
- [16] Yaroshchuk, O., Dumont, M., Zakrevskyy, Yu., Bidna, T., & Lindau, J. (2004). *J. Phys. Chem. B*, 108, 4647.
- [17] Lim, T. K., Hong, S. H., Jeong, M. Y., & Lee, G. J. (1999). *Macromolecules*, 32, 7051.
- [18] Yaroshchuk, O., Sergan, T., Kelly, J., & Gerus, I. (2002). *Jpn. J. Appl. Phys.*, 41(1), 275.
- [19] Puchkov's'ka, G., Reshetnyak, V., Tereshchenko, A., Yaroshchuk, O., & Lindau, J. (1998). *Mol. Cryst. Liq. Cryst.*, 321, 31.